PCCP

PAPER

View Article Online
View Journal



Cite this: DOI: 10.1039/c7cp04694d

# Monitoring thermally induced structural deformation and framework decomposition of ZIF-8 through *in situ* temperature dependent measurements†

Ben Xu, Yingjie Mei, Zhenyu Xiao, Zixi Kang, Rongming Wang and Daofeng Sun *

Received 12th July 2017,
Accepted 8th August 2017

DOI: 10.1039/c7cp04694d

rsc.li/pccp

ZIF-8 is an easily synthesized porous material which is widely applied in gas storage/separation, catalysis, and nanoarchitecture fabrication. Thermally induced atomic displacements and the resultant framework deformation/collapse significantly influence the application of ZIF-8, and therefore, *in situ* temperature dependent FTIR spectroscopy was utilized to study the framework changes during heating in the oxidative environment. The results suggest that ZIF-8 undergoes three transition stages, which are the lattice expansion stage below 200 °C, the "reversible" structural deformation stage from 200 to 350 °C, and the decomposition/collapse stage over 350 °C. Our research indicates that the Zn–N bond breaks at a temperature of 350 °C in the oxidant environment, leading to a drastic deformation of the ZIF-8 structure.

## 1 Introduction

Metal–organic frameworks (MOFs) are constructed by metal or metal clusters bridged by organic ligands, and have large porosity and adjustable pore sizes which are ideal for applications in the fields of gas separation, selective catalysis, and pollutant removal.[1–3] Moreover, MOFs are also utilized as sacrificial precursors for preparing carbon-based or metal-oxide nanomaterials for the applications of electrochemical energy, including lithium-ion batteries, supercapacitors, and fuel cells.[4–8] Zeolitic imidazolate framework-8 (ZIF-8) is one of the most studied MOFs due to its easy synthesis, low-cost raw materials, and high chemical and thermal stability.[9–12] These advantages endow ZIF-8 with the priorities in commercial application compared with other MOF materials. The basic unit of ZIF-8 is a Zn(II)–N tetrahedron bridged by imidazolate rings, and it has the cubic lattice with a space group of $I\bar{4}3m$. The narrow window size of 3.4 Å and the large cavities of 11.4 Å allow ZIF-8 to separate homologues of alkanes and adsorption of small gases.[11,13] Interestingly, the ZIF-8 structure is flexible enough for slow passage of gas molecules with the kinetic sizes larger than the window size (3.4 Å), for example, $O_2$ (3.45 Å), $N_2$ (3.6 Å), and $CH_4$ (3.8 Å).[11,14] Furthermore, it is reported that temperature strongly affects the adsorption and separation capability of ZIF-8,[15–17] which is attributed to the temperature induced structural deformation, along with the chemical changes sometimes. Many characterization techniques including XRD, TGA, and BET are utilized to study the structural, compositional, and morphological changes during heating under different atmospheres, and it is concluded that the thermal stability of ZIF-8 under inert and oxidative environments is quite different. XRD analyses indicate that ZIF-8 remains unchanged at 500 °C in Ar while it transforms to ZnO at 300 °C in air.[16,17] However, most research studies focus only on the structures before and after heating, while neglect the structural changes during heating, which means that the results are less applicable since the studies do not reveal the real working conditions. In order to study the instantaneous alteration during heating, *in situ* measurements are necessary. Therefore, we employed *in situ* temperature dependent FTIR measurements to monitor thermally induced molecular moieties and atomic dislocations in ZIF-8 to investigate its thermal stability. To our knowledge, it is the first time that the *in situ* FTIR technique is reported to monitor thermally induced structural changes of ZIF-8.

Vibrational spectroscopy is widely applied for compositional studies based on the characteristic absorption peaks of vibrational modes of materials, including MOFs.[18,19] The structural deformation due to pressure or temperature usually contributes to small variation in inter-atomic distances, which significantly alters the molecular vibrations and thus can be monitored by vibrational spectroscopy including Raman and FTIR.[13,20,21] In 2011, Hu studied the vibrational modes in ZIF-8 under a high

*State Key Laboratory of Heavy Oil Processing, College of Science, China University of Petroleum (East China), Qingdao, Shandong, 266580, People's Republic of China. E-mail: dfsun@upc.edu.cn*

† Electronic supplementary information (ESI) available. See DOI: 10.1039/c7cp04694d

pressure of up to 39 GPa *via in situ* ATR-FTIR spectroscopy to illustrate the chemical stability and gas-storage capability under extreme compression.[21] By carefully analyzing the changes in peak shapes, peak intensities, and peak positions, he pointed that although ZIF-8 underwent an irreversible structural transition to a disordered or an amorphous phase above a pressure of 1.6 GPa, the chemical composition still remains unchanged even under a pressure over 39 GPa. Kumari studied the temperature effects on ZIF-8 cavity sizes by *in situ* Raman spectroscopy in the temperature range from 77 K to 353 K.[13] The softening of C–H stretching frequencies below 153 K illustrate the decrease in steric hindrance between the methyl groups, contributing to increasing nitrogen and methane uptake at low temperatures. These reports indicate that vibrational spectroscopy is a powerful technique to explore the structure deformation at the molecular level in ZIF-8.

Herein, we investigated the heating effects on the ZIF-8 structure in the temperature range from 25 to 500 °C by *in situ* temperature dependent FTIR measurements along with *off situ* XRD and TGA analysis. DFT calculations were also performed to assign each IR peak to its correlated vibrational mode of ZIF-8. By analyzing the IR peak changes during heating, the structural deformation and framework collapse at the molecular level were studied. Our results provide information about thermally induced structural and chemical variations, which are of significance to the application of ZIF-8 in gas separation/storage.

# 2 Experimental details

## 2.1 Synthesis of ZIF-8 nano crystals

ZIF-8 nano crystals were synthesized based on the reported literature.[21] A 25 mL methanol solution of $Zn(NO_3)_2{\cdot}6H_2O$ (0.3028 g, 1.018 mmol) was rapidly poured into a 25 mL methanol solution of 2-methylimidazole (0.3287 g, 4.004 mmol) at room temperature. The mixture was under stirring with a magnetic bar for 10 minutes until ZIF-8 started to crystallize and remained unchanged for the subsequent 24 hours. The white precipitants were centrifuged and rinsed with methanol three times to remove the solutions and kept at 80 °C overnight.

## 2.2 Calcinating ZIF-8 at different temperatures

Calcinating ZIF-8 powders were conducted using an electrical tubular furnace at temperatures of 200 °C, 250 °C, 300 °C, 350 °C, 400 °C, 450 °C, and 500 °C. The ZIF-8 powders were calcinated in air at each temperature for 5 hours and air cooled to room temperature. The yielded products were checked by XRD to investigate the structural changes.

## 2.3 Characterization methods

TGA measurements were performed by the Mettler Toledo TGA/DSC1 simultaneous thermal analysis. The ZIF-8 powders were heated under the oxygen flow from room temperature to 900 °C with a heating rate of 2 °C per minute. XRD results were obtained utilizing a Rigaku Unlima IV system with Cu Kα radiation. The SEM images were pictured using a Hitachi S-4800 FE-SEM with an applied voltage of 5.0 kV. The FTIR transmission spectra were collected on a PerkinElmer Frontier FTIR spectrometer in the range of 4000–400 $cm^{-1}$ with 2 $cm^{-1}$ resolution. The KBr pellets were prepared for collecting the spectra. The ZIF-8 powders were ground with spectrophotometric grade KBr, pressed into 14 mm diameter pellets under 2 tons, and the resultant pellets were affixed to the stainless mounting stage with thermal epoxy.

*In situ* temperature dependent measurements were conducted using a self-made heating stage (shown in Fig. S1, ESI†). A ceramic heater and a K-type thermocouple (working range from 0 to 900 °C) were attached to the stainless stage as the heating source and detector, and they were both wired to a PDI temperature controller (working range from −199 to 1000 °C) which was used to monitor and control the temperature of the heating stage. During measurements, the heating stage wrapped with thermal insulation was sealed in a box. There is an aperture with diameter 6 mm to allow the IR beam through the whole setup in order to collect the spectra at different temperatures. Heating temperatures were confirmed using a commercial infrared thermometer to ensure that the setup worked at correct temperatures. The pellet was heated from room temperature to 500 °C with an interval of 25 °C and was maintained at each temperature step for 30 minutes before collecting the spectrum.

# 3 Computational details

The electronic structure calculations were carried out using DFT in a plane wave pseudopotential implementation using the CASTEP code in Material Studio.[22–25] The ZIF-8 crystal was built based on the Crystallography Open Database (COD ID: 7111969).[14] As shown in Fig. S2 (ESI†), primary cells with $a = b = c = 14.722$ Å and $\alpha = \beta = \gamma = 109.471°$ with 174 atoms were utilized for the DFT calculations. The exchange–correlating function of GGA-PBE was employed. The SCF tolerance of $1 \times 10^{-3}$ eV per cell was set for convergence. The FFT grid of $96 \times 96 \times 96$ and the Monkhorst–Pack *k*-point of $1 \times 1 \times 1$ was used. Although it is more accurate to set a more precise *k*-point mesh, this was adequate for our purpose. Norm conserving pseudopotentials were used to represent ionic cores, and the pseudopotentials used for hydrogen, carbon, nitrogen, and zinc were H_00PBE_OP.recpot, C_00PBE_OP.recpot, N_00PBE_OP.recpot, and Zn_00.recpot.

# 4 Results and discussion

The as-prepared ZIF-8 nanocrystals with an average size of 100–150 nm presented a typical dodecahedron as shown in Fig. 1(a). The XRD patterns of ZIF-8 powders (Fig. 1(b)) are the same as the simulated result, indicating the successful preparation of ZIF-8. TGA plots are presented in Fig. 1(b). The TGA value remains unchanged from 29 to 210 °C. The subsequent decrease to 91.38% from 210 to 397 °C is mainly due to the partial dissociation of methyl groups.[15] A rapid weight fall from 90% to 52% occurs in the region from 397 to 415 °C, during

 

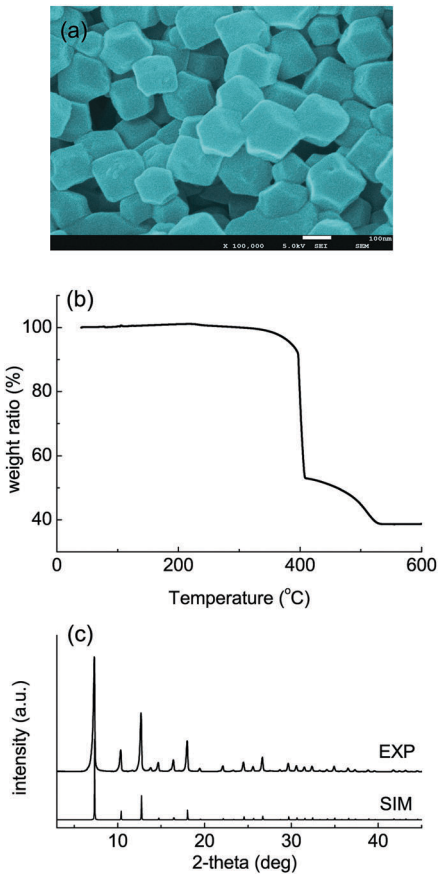


Fig. 1 SEM images of as-prepared ZIF-8 noanocrystals (a), TGA plot of ZIF-8 in the oxygen flow (b), and the PXRD pattern of ZIF-8 powders (c).

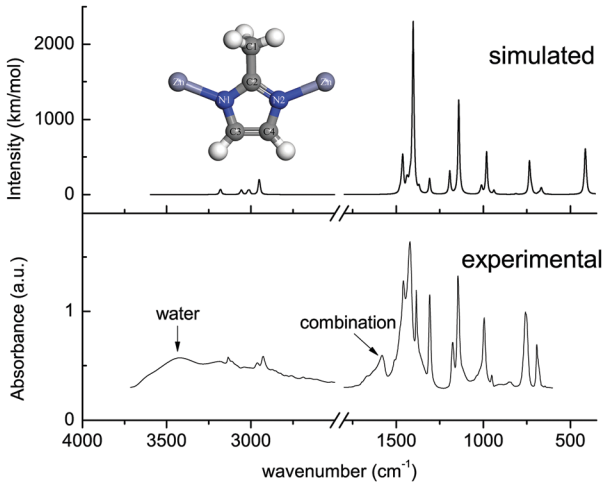


Fig. 2 Simulated and experimental IR spectra of ZIF-8. Two results correspond to each other, indicating the calculation results are reliable. The broad band around 3500 $cm^{-1}$ is due to adsorbed water. The peak at 1560 $cm^{-1}$ is not shown in the simulated spectrum, indicating that it is not the normal vibrational modes of ZIF-8. We suggest it is a combination mode.

which the $CO_x$ and $NO_x$ volatiles form and escape.[7] The step between 415 and 530 °C during which the weight ratio drops from 52% to 39% can be attributed to the formation of zinc oxide.[17] The final weight loss of 60% implies the complete transformation of ZIF-8 (molecular weight of 227.59) to zinc oxide (molecular weight of 81.39) under the oxidative environment.

The TGA results indicate that ZIF-8 remains unchanged below 210 °C, which is similar to previous studies.[26] However, the structural changes contributing to it cannot be studied using TGA. *In situ* temperature dependent FTIR measurements were therefore employed. The IR spectra of ZIF-8 have been widely reported. However, there are still debates on the origination of each IR peak.[13] For example, the peak at 422 $cm^{-1}$ is usually ascribed to the Zn–N stretching mode,[15,21] but some literature indicated that the Zn–N stretching peak is at 273 and 168 $cm^{-1}$. Therefore, DFT calculations were performed in order to correlate the atomic moieties with IR absorption peaks. As shown in Fig. 2, both the experimental (at room temperature) and calculated IR spectra of ZIF-8 were presented. Two results correlated well with each other.

Based on the DFT calculations, the assigned IR peaks to their relevant vibrational modes are listed in Table S1 and Fig. S3 (ESI†). The calculations suggest that the Zn–N stretching mode is at 273 $cm^{-1}$, however, the bending or stretching of the aromatic ring will always lead to changes in the relative position of N to Zn. It is worth mentioning that the 422 $cm^{-1}$ peak is from the bending mode between the methyl group and the imidazolate ring. Two peaks were not observed in the simulated spectrum. One is the broad band around 3400 $cm^{-1}$ due to O–H stretching of water, and the other one is the peak at 1580 $cm^{-1}$, which is probably a combination mode. Some literature assigns this band to C=N stretching, however, our calculations suggest that the C=N stretching mode is at 1307 and 1458 $cm^{-1}$.

The temperature effects on molecular vibrations in ZIF-8 are illustrated in Fig. 3 and Fig. S5 (ESI†). The IR spectra below 200 °C do not show significant differences although slight broadening and lowering in IR peaks are observed, which is due to larger atomic displacements at higher temperatures.[20] Meanwhile, most peaks shift to lower wavenumbers because of the thermal expansion of lattices. In the spectrum collected at 300 °C, the double peaks at 1459 $cm^{-1}$ and 1421 $cm^{-1}$ almost disappear, only a single broad peak centered at 1434 $cm^{-1}$ is present instead. Furthermore, the weak peaks due to the asymmetric stretching of $-CH_3$ (at 2962 $cm^{-1}$ originally) and the aromatic in-plane bending (at 951 $cm^{-1}$ originally) are not observed, which is due to the fact that the flexible C–H bonds are easily affected by the deformation.[13] Decomposition of ZIF-8 can be illustrated by the growth of the peak centered at 2166 $cm^{-1}$, which are assigned to the –C≡N group resulting from the breakage of Zn–N bonds. The –C≡N peak appears at around 400 °C, which corresponds to the TGA results. The spectrum at 500 °C is quite different from others. The significant lowering in ZIF-8 IR peaks and the strong cyano peak at 2166 $cm^{-1}$ suggest the rapid decomposition of ZIF-8, and the drastically broadened bands may correspond to the disordered framework or some unknown amorphous phases. It is worth mentioning that Zn–N bonds are prone to attacks of oxygen, causing lowering of the breaking temperature of 400 °C in air compared with 550 °C in the inert atmosphere.

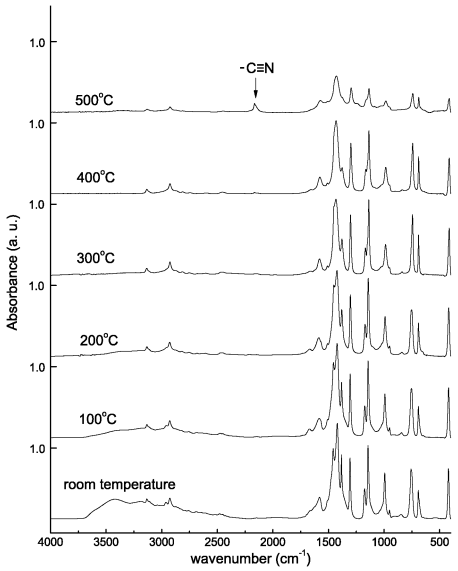


Fig. 3 FTIR spectra of ZIF-8 at different temperatures. The significant drop of IR peaks and the growth of –C≡N peak from 400 to 500 °C indicate the decomposition of ZIF-8. The broaden IR bands for 500 °C spectrum implies the transformation of the crystallized phase to amorphous phases.

To further investigate the structural deformation at the molecular level, peak position changes due to heating are analyzed. It is reported that the methyl groups in ZIF-8 are easily affected by temperature,[15] and thus we firstly studied $CH_3$ stretching and bending mode. As shown in Fig. 4, heating effects on methyl M–H bending are different from that on methyl M–H stretching. From room temperature to 200 °C, the peak due to symmetric M–H stretching at 2927 $cm^{-1}$ shifts to 2929 $cm^{-1}$, while the bending peak shifts from 1307 $cm^{-1}$ to 1304 $cm^{-1}$. This is due to the decreasing distance between the two facing methyl groups, which is attributed to the increasing lattice at higher temperature, hinders the atomic displacement, leading to hardening of the M–H stretching. Meanwhile, the hardening in the stretching mode is accompanied by softening in the bending mode of the methyl group.[13] The correlation between the M–H stretching and bending mode indicates that the ZIF-8 framework remains at temperatures below 200 °C, and the main structural change is the thermally induced expansion, which corresponds to the TGA results. Deformation of ZIF-8 occurs above 200 °C, which is illustrated by the inflections at 225 °C for both curves. Linear fits were performed on the regions below and above 200 °C, marked as red solid lines, and the results (detailed fitted results are listed in Table S2, ESI†) indicate that the peak position changes distinctively at the two temperature regions. Decomposition of ZIF-8 starts at around 400 °C at which peak intensities drastically decrease, as shown in Fig. 4(a) and (c).

Position changes during heating for other peaks are shown in Fig. S4 (ESI†). It is evident that the peak positions for all peaks follow different linear relationships below and above 200 °C, indicating the transition point of 200 °C. It is reported that the adsorbed molecules escape at this temperature,[26] and we believe that the structural deformation is the dominant reason. Collapse or decomposition occurring at around 400 °C is illustrated by the subsequent drop in IR peak intensities, corresponding to the TGA results. As shown in Fig. 5, the –C≡N peak is absent in the spectra below 250 °C, and it remains very weak up to 375 °C. The obvious growth starts from 400 °C. It is clear that the intensities of all ZIF-8 peaks decrease at a higher rate above 400 °C, accompanying the growth of the –C≡N peak. The drastic growth and weakening of the –C≡N and other ZIF-8 peaks above 400 °C implies the rapid decomposition of ZIF-8 and the resultant framework collapse.

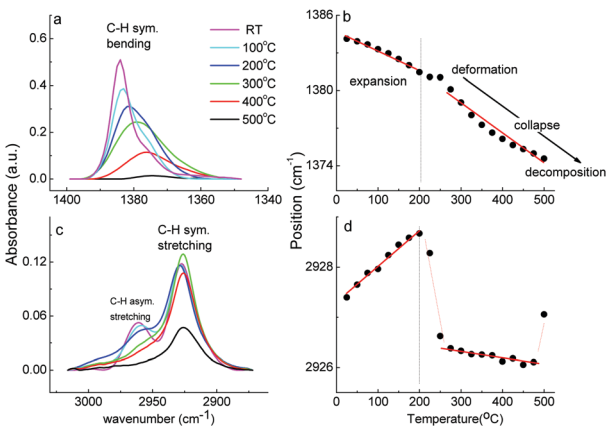


Fig. 4 Temperature effects on C–H bending (a and b) and stretching (c and d) mode of the methyl group. Softening and hardening of the bending and stretching modes below 200 °C indicate the expansion of ZIF-8 with the framework unchanged. Deformation of ZIF-8 framework occurs at 225 °C as shown in (b) and (d).

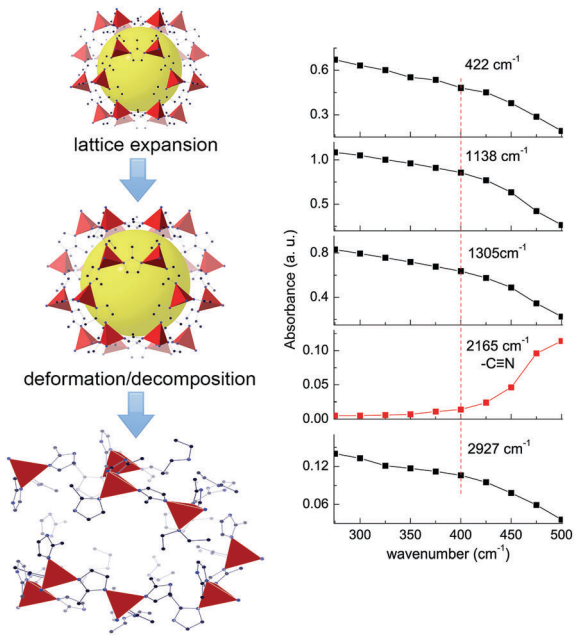


Fig. 5 IR peak intensities are strongly affected by temperature. The 2165 $cm^{-1}$ peak indicating the –C≡N bond appears at 275 °C and rapidly grow above 400 °C, indicating the rapid decomposition of ZIF-8 above 400 °C.

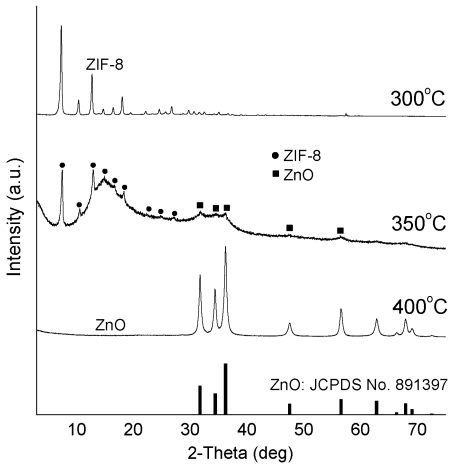


Fig. 6 XRD results for calcined ZIF-8 at different temperatures. Decomposition and transition do not occur until 300 °C. At 350 °C, ZIF-8 slowly transforms to poor crystallized ZnO, and the higher temperature accelerate the formation and crystallization of ZnO.

The results for *off situ* XRD measurements are shown in Fig. 6 and Fig. S6 (ESI†). The ZIF-8 powders were heated at different temperatures and air cooled for PXRD measurements. Unlike the *in situ* FTIR results, which suggest that the structure deforms at 200 °C, the XRD pattern for ZIF-8 remains unchanged up to 300 °C. Therefore, we can conclude that the structural deformation occurring between 200 °C and 300 °C is reversible after cooling. However, the structure cannot be cured if the heating temperature is maintained at 350 °C. At this temperature, ZIF-8 powders are slowly transformed to poorly crystallized ZnO, and the bumpy background is possible due to some amorphous phases. The fast transformation of ZIF-8 to well crystallized ZnO is illustrated by the strong and sharp ZnO peaks presented in the XRD pattern for 400 °C, which corresponds to the *in situ* FTIR results.

Previous studies have pointed that the annealing of ZIF-8 in an inert atmosphere will preferentially break the methyl-imidazolate connections due to the smaller dissociation enthalpy of the methyl-imidazolate bond. Furthermore, it is found that the ZIF-8 framework remains with the dissociation of the $-CH_3$ group.[15] Their findings can explain our *in situ* FTIR results to some extent. We noticed that the asymmetric methyl C–H stretching mode almost disappears at 300 °C, and it can be attributed to the easy dislocation of methyl groups at higher temperature. However, we did not find the evidence indicating the preferential dissociation of the methyl group or Zn–N bonds. The growth of the $-C\equiv N$ peak is accompanied by the overall weakening of the IR spectrum, implying the simultaneous breaking of methyl-imidazolate bonds, Zn–N bonds, and imidazolate bonds. We also noticed that the drastic weakening of the ZIF-8 IR peak occurs at a temperature of 400 °C, which is lower than the decomposition temperature in the inert atmosphere.[17] Therefore, we suggest that the oxidant environment promotes the breaking of imidazolate rings.

Based on our studies, ZIF-8 experiences three transition stages during heating in the oxidant environment, which are: (1) dislocation of methyl groups below 200 °C during which the framework remains unchanged, and the thermal expansion is the main change in the ZIF-8 lattice; (2) further dislocation of methyl groups below 300 °C leading to revisable deformation (cured once cooled); and (3) collapse of the ZIF-8 framework occurs at a temperature higher than 350 °C, and rapid transformation to ZnO occurs at 400 °C and above.

## 5 Conclusions

Overall, our investigation provides a deep insight into the heating effects on ZIF-8 at the molecular level. *In situ* temperature dependent FTIR measurements were conducted along with other methods including XRD, TGA, and DFT calculations to study the heating effects on the ZIF-8 structure in the oxidant atmosphere. By monitoring the atomic moieties during heating using the *in situ* FTIR technique and investigating the structural and chemical changes after heating using XRD, it is concluded that there are three stages during the transformation of ZIF-8 to ZnO in air. The first stage is below 200 °C where the ZIF-8 structure does not deform, while a slight lattice expansion occurs. Above 200 °C, the ZIF-8 framework does not maintain its original shape, although this deformation is reversible after cooling until the temperature is above 300 °C. Decomposition occurs at the last stage above 350 °C, and higher temperature attributes to faster transformation of ZIF-8 to crystallized ZnO in air.

Our results are of significance to the application of ZIF-8 at high temperatures. ZIF-8 has been widely used for gas storage, separation, and nanoarchitecture fabrication by calcining it. Although the framework of ZIF-8 can be well maintained after cooling from 300 °C, it is not appropriate to use ZIF-8 at temperatures above 200 °C where the framework actually deforms, especially for gas separation/storage in which the capabilities are strongly dependent on the cavity and tunnel sizes in the framework. We suggest that thorough and deep studies will be needed to explore the structural transitions and transformation during heating ZIF-8 to guide its application at high temperatures.

## Conflicts of interest

There are no conflicts to declare.

## Acknowledgements

We are grateful for financial support from the National Natural Foundation of China (Grant No. 21371179, 21571187 and 21501198), the Taishan Scholar Foundation (ts201511019), and the Fundamental Research Funds for the Central Universities (16CX02016A).

## References

1 O. M. Yaghi, H. Li and T. L. Groy, *J. Am. Chem. Soc.*, 1996, **118**, 9096–9101.

2 O. K. Farha, A. Ö. Yazaydn, I. Eryazici, C. D. Malliakas, B. G. Hauser, M. G. Kanatzidis, S. T. Nguyen, R. Q. Snurr and J. T. Hupp, *Nat. Chem.*, 2010, **2**, 944–948.
3 Z. Kang, L. Fan and D. Sun, *J. Mater. Chem. A*, 2017, **5**, 10073–10091.
4 X. Zhang, J. Luo, P. Tang, X. Ye, X. Peng, H. Tang, S.-G. Sun and J. Fransaer, *Nano Energy*, 2017, **31**, 311–321.
5 S. Tang, B. Zhu, X. Shi, J. Wu and X. Meng, *Adv. Energy Mater.*, 2017, **7**, 1601985.
6 H. Tabassum, A. Mahmood, Q. Wang, W. Xia, Z. Liang, B. Qiu, R. zhao and R. Zou, *Sci. Rep.*, 2017, **7**, 43084.
7 Y. V. Kaneti, J. Tang, R. R. Salunkhe, X. Jiang, A. Yu, K. C.-W. Wu and Y. Yamauchi, *Adv. Mater.*, 2017, **29**, 1604898.
8 P. C. Shi, J. D. Yi, T. T. Liu, L. Li, L. J. Zhang, C. F. Sun, Y. B. Wang, Y. B. Huang and R. Cao, *J. Mater. Chem. A*, 2017, **5**, 12322–12329.
9 T. T. Isimjan, H. Kazemian, S. Rohani and A. K. Ray, *J. Mater. Chem.*, 2010, **20**, 10241–10245.
10 N. L. Torad, M. Hu, Y. Kamachi, K. Takai, M. Imura, M. Naito and Y. Yamauchi, *Chem. Commun.*, 2013, **49**, 2521–2523.
11 T. Yang and T.-S. Chung, *Int. J. Hydrogen Energy*, 2013, **38**, 229–239.
12 Y. Huang, Y. Zhang, X. Chen, D. Wu, Z. Yi and R. Cao, *Chem. Commun.*, 2014, **50**, 10115–10117.
13 G. Kumari, K. Jayaramulu, T. K. Maji and C. Narayana, *J. Phys. Chem. A*, 2013, **117**, 11006–11012.
14 O. Shekhah, R. Swaidan, Y. Belmabkhout, M. du Plessis, T. Jacobs, L. J. Barbour, I. Pinnau and M. Eddaoudi, *Chem. Commun.*, 2014, **50**, 2089–2092.
15 H. Huang, W. Zhang, D. Liu, B. Liu, G. Chen and C. Zhong, *Chem. Eng. Sci.*, 2011, **66**, 6297–6305.
16 S. Gadipelli, W. Travis, W. Zhou and Z. Guo, *Energy Environ. Sci.*, 2014, **7**, 2232–2238.
17 H. Yin, H. Kim, J. Choi and A. C. Yip, *Chem. Eng. J.*, 2015, **278**, 293–300.
18 C. Petit and T. J. Bandosz, *J. Mater. Chem.*, 2009, **19**, 6521–6528.
19 J. Gascon, M. D. Hernández-Alonso, A. R. Almeida, G. P. van Klink, F. Kapteijn and G. Mul, *ChemSusChem*, 2008, **1**, 981–983.
20 B. Xu and K. M. Poduska, *Phys. Chem. Chem. Phys.*, 2014, **16**, 17634–17639.
21 Y. Hu, H. Kazemian, S. Rohani, Y. Huang and Y. Song, *Chem. Commun.*, 2011, **47**, 12694–12696.
22 P. Hohenberg and W. Kohn, *Phys. Rev.*, 1964, **136**, B864–B871.
23 W. Kohn and L. J. Sham, *Phys. Rev.*, 1965, **140**, A1133–A1138.
24 M. C. Payne, M. P. Teter, D. C. Allan, T. Arias and J. D. Joannopoulos, *Rev. Mod. Phys.*, 1992, **64**, 1045–1097.
25 B. G. Pfrommer, M. Cote, S. G. Louie and M. L. Cohen, *J. Comput. Phys.*, 1997, **131**, 233–240.
26 T. Lee, H. Kim, W. Cho, D.-Y. Han, M. Ridwan, C. W. Yoon, J. S. Lee, N. Choi, K.-S. Ha and A. C. Yip, *et al.*, *J. Phys. Chem. C*, 2015, **119**, 8226–8237.

 